R_s with sputter etching detected in that study was also observed in the present study.[4] However, this was suggested to arise from preferential sputtering of Si[4] (compared to Al), rather than the exposure of selective layer structures.[6] The former conclusion was reached because the R_s following sputtering eventually dropped substantially below R_b. The counter arguments of Dwyer et al., however, cannot be ruled out.[6] In addition, one should not preclude differences resulting from the choice of distinctly different sputter etching energies and other conditions. The excellent reproducibility achieved by Dwyer et al.[6] employing bombardment techniques is a persuasive feature in their arguments and may counter any criticism of the quantitation of these techniques. The present results agree with a number of Dwyer's hypotheses. The present study also provides possible chemical identifications of the mixtures formed at zeolite surfaces. Additional, better-coordinated studies are needed, however, in order to establish the interconnections between these two approaches.

In general, it may be concluded that the *surfaces of certain zeolites are compromised such that substantial proportions of their total surface (Al) are actually present in alumina or sodium aluminate residues*. Note that since the Si/Al ratio (R_s) reported in most previous ESCA studies does not reflect the substantial presence of these nonzeolitic residues, the (R_s) of *true* zeolites may actually be much larger than these reported values.

UV Resonance Raman Excitation Profiles of the Aromatic Amino Acids

Sanford A. Asher,* Michael Ludwig, and Craig R. Johnson

Contribution from the Department of Chemistry, University of Pittsburgh, Pittsburgh, Pennsylvania 15260. *Received September 5, 1985*

Abstract: The first total differential resonance Raman cross-section excitation profiles have been measured throughout an electronic transition of a simple aromatic molecule. The excitation profiles of the aromatic amino acids phenylalanine, tyrosinate, and tryptophan were measured between 217 and 600 nm. The mechanism for resonance enhancement for each of these benzene derivatives is discussed. The ν_1 symmetric ring stretch at 750 cm^{-1} in phenylalanine derives its preresonance enhancement from the $B_{a,b}$ transitions, while the other vibrations are enhanced by the L_a transition at ca. 210 nm. The excitation profiles for tyrosinate indicate that the L_a state has little charge-transfer character, while the L_b and states further in the UV have significant charge-transfer character. The excitation profile data are used to assign the resonance enhanced vibrations. The relationship between resonance enhancement of a vibrational mode, the atomic displacements in the vibration, and the molecular electronic transition is examined. The cross sections are used to determine the optimal excitation wavelength required to selectively enhance particular aromatic amino acids in proteins. The resonance Raman spectra of lysozyme are discussed. Photochemical and optical saturation processes which commonly occur with pulsed laser excitation can change the apparent contributions of aromatic amino acid intensities in the Raman spectra. Transient species can also form and alter the measured Raman spectra. These processes can cause artifactual Raman spectral changes.

Recently, a number of reports have appeared on the use of UV resonance Raman (UVRR) spectroscopy as a new probe for studying both the excited states[1-14] and the ground states of molecular species.[15-22] A major inducement for some of these UV spectral measurements is the potential utility of UVRR spectroscopy as a new technique for the study of biomolecular structure and function.[15,19-22] Indeed, recent UVRR investigations of aromatic amino acids, proteins, and model peptide compounds have clearly illustrated the potential of UVRR spectroscopy. These studies indicate that selective enhancement of protein aromatic amino acids is possible.[19,22] Other studies suggest that peptide backbone vibrations can be selectively enhanced with ca. 190-nm excitation.[4,11,22] A major revolution in insight accompanied visible wavelength RR studies of the mechanism of energy transduction in the visual pigments[23,24] and the mechanism of ligand binding and the structure and function in heme proteins.[23-26] Similar important strides are expected with the application of UV Raman spectroscopy to the structure, bonding, and intermolecular interactions of aromatic amino acids in proteins.

In this report we carefully characterize the UV resonance Raman excitation profiles of aqueous solutions of phenylalanine, tyrosinate, and tryptophan from 217 to 600 nm. We also discuss and review some of the photophysics which accompany UV pulsed laser excitation in these molecules.[6,27] The excitation profiles indicate the selectivity available for resonance Raman excitation of a particular type of aromatic amino acid. The detailed excitation profile patterns can be used to obtain information about the excited state. The degree of enhancement of a vibration is intimately related to the molecular electron density differences

* Author to whom correspondence should be addressed.

(1) Asher, S. A.; Johnson, C. R.; Murtaugh, J. *Rev. Sci. Instrum.* **1983**, *54*, 1657.
(2) Asher, S. A.; Johnson, C. R. *J. Phys. Chem.* **1985**, *89*, 1375.
(3) Dudik, J. M.; Johnson, C. R.; Asher, S. A. *J. Chem. Phys.* **1985**, *82*, 1732.
(4) Dudik, J. M.; Johnson, C. R.; Asher, S. A. *J. Phys. Chem.* **1985**, *89*, 3805.
(5) Jones, C. M.; Johnson, C. R.; Asher, S. A.; Shepherd, R. E. *J. Am. Chem. Soc.* **1985**, *107*, 1372.
(6) Johnson, C. R.; Ludwig, M.; Asher, S. A. *J. Am. Chem. Soc.* **1986**, *108* 905.
(7) Ziegler, L. D.; Hudson, B. S. *J. Chem. Phys.* **1981**, *74*, 982.
(8) Ziegler, L. D.; Hudson, B. S. *J. Chem. Phys.* **1983**, *79*, 1134.
(9) Ziegler, L. D.; Hudson, B. S. *J. Phys. Chem.* **1984**, *88*, 1110.
(10) Ziegler, L. D.; Hudson, B. S. *J. Chem. Phys.* **1983**, *79*, 1197.
(11) Mayne, L. C.; Ziegler, L. D.; Hudson, B. *J. Phys. Chem.* **1985**, *89*, 3395.
(12) Ziegler, L. D.; Kelley, P. B.; Hudson, B. *J. Chem. Phys.* **1984**, *81*, 6399.
(13) Gerrity, D. P.; Ziegler, L. D.; Kelley, P. B.; Desiderio, R. A.; Hudson, B. *J. Chem. Phys.*, in press.
(14) Korenowski, G. M.; Ziegler, L. D.; Albrecht, A. C. *J. chem. Phys.* **1978**, *68*, 1248.
(15) Jones, C. M.; Naim, T.; Ludwig, M.; Murtaugh, J.; Flaugh, P. F.; Dudik, J. M.; Johnson, C. R.; Asher, S. A. *Trends Anal. Chem.* **1985**, *4*, 75.
(16) Asher, S. A. *Anal. Chem.* **1984**, *56*, 720.
(17) Asher, S. A.; Johnson, C. R. *Science (Washington, D. C.)* **1984**, *225*, 311.
(18) Johnson, C. R.; Asher, S. A. *Anal. Chem.* **1984**, *56*, 2258.
(19) Johnson, C. R.; Ludwig, M.; O'Donnell, S. E.; Asher, S. A. *J. Am. Chem. Soc.* **1984**, *106*, 5008.
(20) Fodor, S. P. A.; Rava, R. P.; Hays, T. R.; Spiro, T. G. *J. Am. Chem. Soc.* **1985**, *107*, 1520.

0002-7863/86/1508-3186$01.50/0

between the ground and excited state and the particular nuclear displacements which occur for the vibrational mode.[3,4] From the excitation profiles we detect and assign the underlying vibronic structure in the absorption bands of each of the aromatic amino acids and assign the vibrational modes.

The results here indicate that all previously reported UV resonance Raman studies of tryptophan and tyrosine either in solution or in proteins[19,21,22] may suffer from photochemical[6] and optical artifacts.[27] Any UV Raman spectral data obtained using pulsed laser excitation sources must be carefully examined to ensure that the spectra derive from ground-state molecules unperturbed by the pulsed laser excitation. For tryptophan residues, this will require especially careful excitation power dependence studies.[27]

Experimental Section

Samples of tryptophan, phenylalanine, and tyrosine obtained from Sigma Chemical Co. (St. Louis, MO) were prepared as aqueous solutions at pH 11.5 to ensure that the amino acids were fully deprotonated. The Raman spectra of the solutions were measured in a flowing closed cycle recirculating stream in which the solutions were pumped through a 1.0 mm internal diameter Suprasil quartz capillary tube. The scattered light was collected at 90°.

The Raman spectrometer has been described in detail elsewhere.[1,28] The excitation source is a Quanta-Ray DCR-2A Nd-YAG laser operated at 20 Hz and frequency doubled to pump a dye laser. UV light is generated by either doubling the dye laser frequency or by mixing the doubled frequency with the 1.06-μm fundamental of the YAG laser. An ellipsoidal mirror was used to collect the scattered light to avoid chromatic aberrations. The polarization of the scattered light was randomized by a crystalline quartz wedge to avoid intensity artifacts deriving from any polarization efficiency bias of the monochromator. The scattered light was detected with a Princeton Applied Research OMA II system which utilized a Model 1420 blue-enhanced intensified Reticon detector.

The throughput efficiency of the monochromator in the UV was calibrated by using a standard intensity deuterium lamp scattered from a Lambert surface prepared from Kodak White Reflectance Standard. The excitation profile data are derived from peak height measurements. Because the peak shapes and bandwidths of the internal standard and the aromatic amino acids are similar and because the observed peak widths are dominated by the spectrograph slit width, the peak height ratios between the aromatic amino acids and the internal standard are proportional, with negligible error, to the peak integral ratios.[29] The total differential Raman cross section ($d\sigma/d\Omega$) of tryptophan, phenylalanine, and tyrosinate at each excitation wavelength was calculated from the known cross section of perchlorate; we recently determined the Raman cross section of sodium perchlorate as well as other substances commonly used as intensity standards in Raman measurements, including acetonitrile, sodium sulfate, and sodium nitrate.[3]

The excitation profile data were not corrected for sample self-absorption because we have empirically demonstrated that this error is small compared to the standard deviation of the excitation profile data. The maximum spectral difference between the aromatic amino acid and internal standard peak is ca. 700 cm^{-1} which corresponds to only 4 nm at 240 nm. The breadth of the absorption bands ensures that only a small error occurs by neglecting self-absorption. This is especially true in the case where a diffuse, ca. 1-mm-diameter laser beam is the source for the Raman scattered light. No analytical expression for the self-absorption correction is presently known for the complex geometry associated with 90° scattering from a cylindrical flow stream. Sample calculations which overestimate the self-absorption error by assuming an average path length result in a *maximum* likely error of less than 20% for the worst point in the excitation profiles of tyrosinate. Negligible error (<5%) occurs for phenylalanine. For tryptophan the error due to saturation phenomena[27] dominates all other errors in the excitation profile data.

The 10-mL samples of the aromatic amino acids at concentrations of 1–6 mM used for the Raman measurements were irradiated for a maximum of 15 min using less than 0.5 mJ/pulse at a pulse repetition rate of 20 Hz. UV absorption spectra of the solutions were measured before and after the Raman measurements to ensure that no significant photochemical decomposition occurred. The laser beam was defocused to minimize the power density in the sample in order to minimize nonlinear optical processes and to avoid the formation of high concentrations of photochemical transients. Under the conditions used, the Raman intensity was found to increase linearly in proportion to the incident intensity for phenylalanine and tyrosinate. The occurrence of optical saturation phenomena was unavoidable for the tryptophan excitation profiles at the powers required to measure the Raman spectra. Depolarization ratios were measured at selected wavelengths by using a Polacoat analyzer.

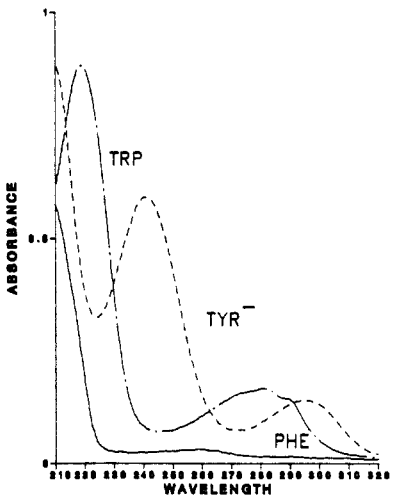

Figure 1. Absorption spectra of aqueous solutions (pH 11.5) of the aromatic amino acids. Concentrations: 2.5×10^{-5} M tryptophan; 5.3×10^{-5} M tyrosinate; 1.5×10^{-4} M phenylalanine. A 1-cm path length was used.

Table I. UV Absorption Spectral Data for Aromatic Amino Acids and Related Compounds[a]

	L_a		L_b	
	λ_{max}, nm	ϵ, M^{-1} cm^{-1}	λ_{max}, nm	ϵ, M^{-1} cm^{-1}
benzene	204	7400	255	200
toluene	206	7000	261	225
phenylalanine	205	9600	258	190
phenol	210	6200	270	1450
p-cresol	220	5400	276	1730
tyrosine	222	9000	275	1400
phenolate	235	9400	287	2600
tyrosinate	240	11000	293	2300
	L_a		L_b	
	λ_{max}, nm	ϵ, M^{-1} cm^{-1}	λ_{max}, nm	ϵ, M^{-1} cm^{-1}
indole	225	25000	270	6000
tryptophan	220	36000	280	5500

[a] Data from ref 30–32.

Results

The absorption spectra of phenylalanine, tyrosinate, and tryptophan are shown in Figure 1. Table I lists spectral data for these and other aromatic molecules of similar structure. For benzene the two lowest energy electronic transitions are symmetry forbidden and involve the B_{1u} and B_{2u} excited states.[33a] Similar $\pi \rightarrow \pi^*$ transitions occur in substituted benzene derivatives where they are denoted as transitions to the L_a and L_b excited states,

(21) (a) Rava, R. P.; Spiro, T. G. *J. am. Chem. Soc.* **1984**, *106*, 4062. (b) Rava, R. P.; Spiro, T. G. *J. Phys. Chem.* **1985**, *89*, 1856.
(22) (a) Rava, R. P.; Spiro, T. G. *Biochemistry* **1985**, *24*, 1861. (b) Copeland, R. A.; Dasgupta, S.; Spiro, T. G. *J. Am. Chem. Soc.* **1985**, *107*, 3370.
(23) Carey, P. R. *Biological Applications of Raman and Resonance Raman Spectroscopies*; Academic: New York, 1982.
(24) Tu, A. T. *Raman Spectroscopy in Biology: Principles and Applications*; Wiley: New York, 1982.
(25) Asher, S. A. *Methods Enzymol.* **1981**, *76*, 371.
(26) Spiro, T. G. In *The Porphyrins*; Lever, A. B. P., Gray, H. B., Eds.; Addison-Wesley: Reading, MA, 1983; Part II, p 89.
(27) Jones, C. M.; Ludwig, M.; Asher, S. A. to be submitted for publication in *Appl. Spectrosc.*
(28) Asher, S. A. *Appl. Spectrosc.* **1984**, *38*, 276.
(29) Murtaugh, J. M.; Asher, S. A. submitted for publication in *Appl. Spectrosc.*
(30) (a) Doub, L.; Vandenbelt, L. D. *J. Am. Chem. Soc.* **1947**, *69*, 2714. (b) Urano, K.; Kawamoto, K.; Hayashi, K. *Yosui to Haisui* **1981**, *23*, 196.
(31) Edelhoch, H. *Biochemistry* **1967**, *6*, 1948.
(32) Weinryb, I.; Steiner, R. F. In *Excited States of Proteins and Nucleic Acids*; Steiner, R. F., Weinryb, I., Eds.; Plenum: New York, 1971; p 277.
(33) (a) Ziegler, L. D.; Hudson, B. S. In *Excited States*; Lim, E. C., Ed.; Academic: New York, 1982; Vol. V, p 41. (b) Platt, J. K.; Klevens, H. B. *Chem. Rev.* **1947**, *41*, 301.

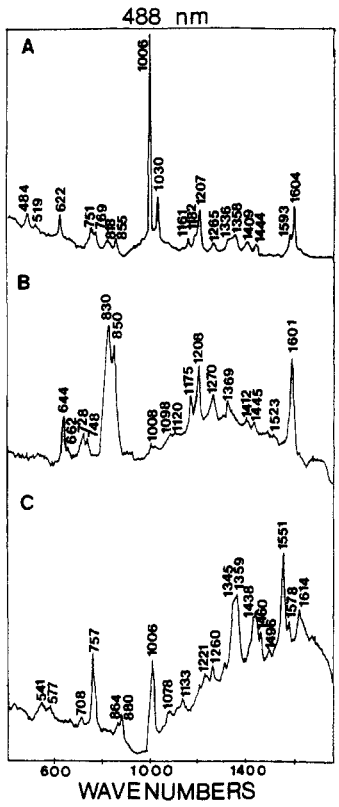

Figure 2. Raman spectra of 0.1 M aqueous solutions of (A) phenylalanine, (B) tyrosinate, and (C) tryptophan excited at 488 nm using a CW laser with 0.9 W of power. All solutions were at pH 11.5. The spectrometer band-pass is 2.5 cm^{-1}. Sloping backgrounds and the Raman bands of water (1640 cm^{-1}) have been subtracted.

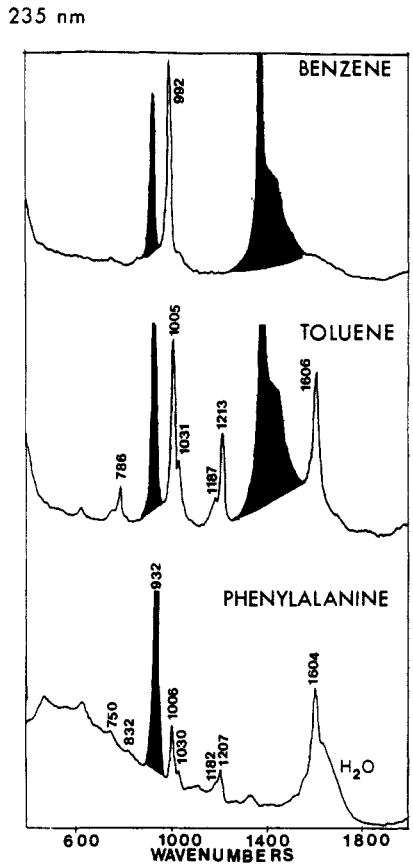

Figure 3. Resonance Raman spectra excited at 235 nm of benzene and toluene in acetonitrile and of an aqueous solution of phenylalanine (0.005 M) containing 0.2 M sodium perchlorate. The acetonitrile and perchlorate peaks are shaded. Power = 0.5 mJ/pulse. Spectra were obtained in 15-min scans.

respectively. As the symmetry of the aromatic ring is decreased by substituents, the forbidden character of these transitions decreases and the oscillator strength increases.[33a,b]

The L_a absorption maximum of phenylalanine occurs at 205 nm with a molar absorptivity of 9600 M^{-1} cm^{-1}, and the L_b band occurs at 258 nm with a molar absorptivity of 190 M^{-1} cm^{-1}. The absorption spectra of phenylalanine and toluene are very similar. Similar absorption spectra are observed for tyrosine, *p*-cresol, and phenol.[30a,b] In contrast, deprotonation of the phenolic hydrogen shifts the L_a absorption maximum from 222 (tyrosine) to 240 nm (tyrosinate). This shift in energy makes it possible to measure the Raman excitation profiles through the entire L_a electronic transition of tyrosinate with available tunable laser excitation sources. The L_a absorption maximum of tyrosinate (Figure 1) occurs at 240 nm with a molar absorptivity of 11 000 M^{-1} cm^{-1}, while the L_b maximum occurs at 293 cm^{-1} with a molar absorptivity of 2300 M^{-1} cm^{-1} (ref 32). The absorption spectrum of tryptophan (Figure 1) shows its first $\pi \rightarrow \pi^*$ absorption band at 280 nm. This band, which has a maximum molar absorptivity of 5500 M^{-1} cm^{-1}, derives from overlapping L_a- and L_b-like $\pi \rightarrow \pi^*$ transitions.[32] A much stronger $\pi \rightarrow \pi^*$ transition with a molar absorptivity of 36000 M^{-1} cm^{-1} occurs at 220 nm.

The normal Raman spectra of phenylalanine, tryosinate, and tryptophan excited at 488 nm (Figure 2) show peaks which derive from the vibrations of both the aromatic side chains and the α-aminocarboxyl group. The assymetric stretch of the ionized carboxyl group[34,35] (ca. 1600 cm^{-1}) is obscured by ring modes in each of the aromatic amino acid spectra. The symmetric stretch of the ionized carboxyl group appears at 1409 and 1412 cm^{-1} in phenylalanine and tyrosinate, respectively.[34] This band is obscured by ring vibrations in the normal Raman spectrum of tryptophan (Figure 2C). Other Raman peaks observed with visible wavelength excitation also derive from vibrational modes localized in the α-aminocarboxyl substituent. In contrast, Raman spectra measured with UV excitation in resonance with the L_a absorption bands show enhancement only of vibrations localized in the aromatic rings of the aromatic amino acids (vide infra).

The resonance Raman spectra of benzene, toluene, and phenylalanine excited at 235 nm are shown in Figure 3. The shaded peaks at 918 and 1376 cm^{-1} in the benzene and toluene spectra derive from the solvent acetonitrile, while the shaded peak at 932 cm^{-1} in the Raman spectrum of phenylalanine derives from the perchlorate internal intensity standard. The Raman peaks are assigned by comparing the phenylalanine Raman spectrum to that of benzene and toluene. The 992-cm^{-1} a_{1g} benzene symmetric ring breathing mode (ν_1), which is intense for Raman spectra excited in the visible spectral region, totally dominates the benzene Raman spectra for resonance close to the B_{1u} transition[2] between 217 and 260 nm. Excitation further into the UV is reported to result in a decreased ν_1 enhancement, especially for 200-nm excitation in gas-phase benzene.[7,13] The 1005-cm^{-1} and 1006-cm^{-1} bands in tolune and phenylalanine *do not* derive from the ν_1 benzene symmetric ring breathing mode, but rather they result from the ν_{12} (b_{1u}) benzene ring breathing mode. Although the qualitatively similar intensities for the 992-cm^{-1} benzene and 1006-cm^{-1} toluene and phenylalanine peaks suggest similar assignments,[8,21] the decrease in ring symmetry to C_{2v} in toluene and phenylalanine results in extensive mode mixing. The ν_1 peak actually occurs at 786 and 750 cm^{-1} in toluene and phenylalanine, respectively.[36]

(34) Lord, R. C.; Yu, N.-T. *J. Mol. Biol.* **1970**, *50*, 509.
(35) Siamwiza, M. N.; Lord, R. C.; Chen, M. C.; Tadahiska, T.; Harada, I.; Matsuura, H.; Shimanouchi, T. *Biochemistry* **1975**, *14*, 4870.

(36) (a) Duinker, J. C.; Mills, I. M. *Spectrochim. Acta, Part A* **1968**, *24A*, 417. (b) Shimanouchi, T. In *Table of Molecular Vibrational Frequencies*; NSRDS-Nat'l Bureau of Standards: Washington, DC, 1972 Vol. I, p 39. (c) Dollish, F. R.; Fateley, W. G.; Bentley, F. F. *Characteristic Raman Frequencies of Organic Compounds*, Wiley: New York, 1974. (d) Kohlrausch, K. W. F. *Raman Spektren*; Heyden and Son: London, 1943. (e) Fuson, N.; Garrigou-Lagrange, G.; Josien, M. L. *Spectrochim. Acta* **1960**, *16*, 106. (f) Jakobsen, R. J. *Spectrochim. Acta* **1965**, *21*, 433.

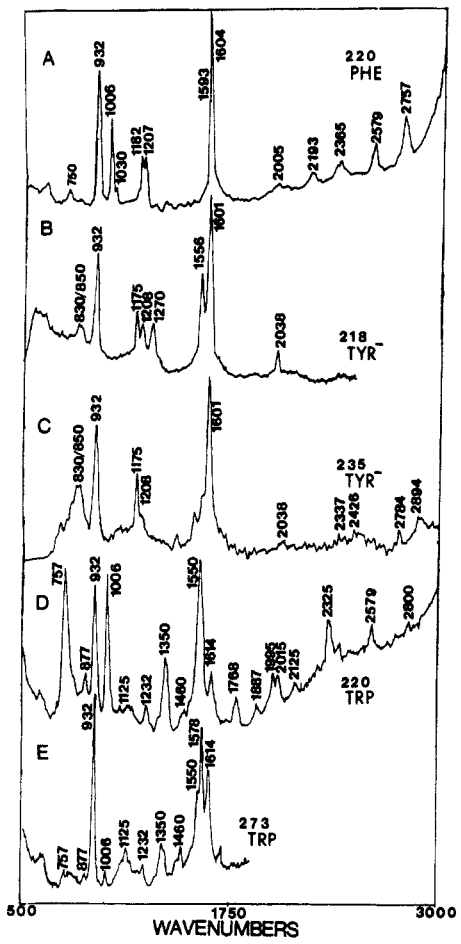

Figure 4. Resonance Raman spectra of aqueous solutions of the aromatic amino acids. (A) Phenylalanine (3 mM) at pH 11.5 containing perchlorate (0.2 M). Excitation wavelength = 220 nm. Power = 0.35 mJ/pulse. Spectral resolution = ca. 13 cm^{-1}. (B) Tyrosinate (5 mM) at pH 11.5 with sodium perchlorate (1.0 M). Excitation wavelength = 218 nm. Power = 0.3 mJ/pulse. Spectral resolution = ca. 14 cm^{-1}. (C) Tyrosinate (5.0 mM) with sodium perchlorate (1.0 M) at pH 11.5. Excitation wavelength = 235 nm. Power = 0.3 mJ/pulse. Spectral resolution = ca. 12 cm^{-1}. (D) Tryptophan (1.0 mM) with sodium perchlorate (1.0 M) at pH 11.5. Excitation wavelength = 220 nm. Power = 0.3 mJ/pulse. Spectral resolution = ca. 14 cm^{-1}. (E) Tryptophan (3.0 mM) with sodium perchlorate (1.0 M) at pH 11.5. Excitation wavelength = 273 nm. Power = 2 mJ/pulse. Spectral resolution = ca. 10 cm^{-1}. The 932-cm^{-1} peak derives from perchlorate.

The ca. 1030-cm^{-1} peaks result from the ν_{18a} C–H bending vibrations[36d] (however, see ref 36e). The bands at ca. 1185 cm^{-1} are in-plane CH deformations (ν_{9a}). The ca. 1210-cm^{-1} bands involve symmetric stretches of the C–C_6H_5 bonds (ν_{7a}). In benzene, the intensity of the degenerate ν_8 e_{2g} vibration (ca. 1600 cm^{-1}) due to ring carbon double bond stretching is vanishingly weak, especially for excitation in the UV.[2,7,13] In contrast, the decreased ring symmetry in phenylalanine and toluene breaks the degeneracy of the ν_8 vibration and results in intense ν_{8a} and ν_{8b} doublets which are observed in the Figure 3 spectra as ca. 1605-cm^{-1} peaks. The ν_{8a} and ν_{8b} bands lie close to frequency and are not separately resolved in the Figure 3 Raman spectra. The strong enhancement of the ν_{8a} and ν_{8b} bands in substituted benzene derivatives with excitation close to the L_a transition was noted earlier by Ziegler and Hudson.[8] The shoulder at ca. 1650 cm^{-1} in phenylalanine derives from water Raman scattering.

The Raman spectrum of phenylalanine excited at 220 nm (Figure 4A) displays a number of combination and overtone bands. Although overtone and combination bands are not commonly observed in normal Raman spectroscopy, strong overtone enhancement has been repeatedly noted with resonance excitation in benzene derivatives.[2,7,8,13] The observed fundamentals, combinations, and overtones of benzene and toluene are tabulated in Table II, while Table III tabulates the Raman peaks, assignments,

(37) Wilson, E. B. *Phys. Rev.* **1934**, *45*, 706.

Table II.[a] Raman Bands of Benzene[b] and Toluene[c]

frequency, cm^{-1}	assignment (symmetry)	description
	Benzene Fundamentals	
606	ν_6 (e_{2g})	in-plane ring deformation
849	ν_{10} (e_{1g})	out-of-plane CH bend
992	ν_1 (a_{1g})	ring breathing
1178	ν_9 (e_{2g})	in-plane CH bend
1326	ν_3 (a_{2g})	in-plane CH bend
1606	ν_8 (e_{2g})	in-plane ring stretch
3047	ν_7 (e_{2g})	in-plane CH stretch
3062	ν_2 (a_{1g})	symmetric in-plane CH stretch
	Toluene Fundamentals	
786	ν_1	symmetric ring breathing
1002	ν_{12}	symmetric ring stretch from benzene b_{1u} vibration
1031	ν_{18a}	in-plane CH bend
1187	ν_{9a}	in-plane CH bend
1212	ν_{7a}	methyl-ring stretching
1606	ν_{8a}	in-plane ring stretching
	Overtones and Combinations	
2608	$\nu_{8a} + \nu_{12}$	
2783	$\nu_{8a} + \nu_{9a}$	
3212	$2\nu_{8a}$	

[a] Mode numbering from ref 37. [b] Assignments from ref 36a–c. [c] Assignments from ref 36c–e.

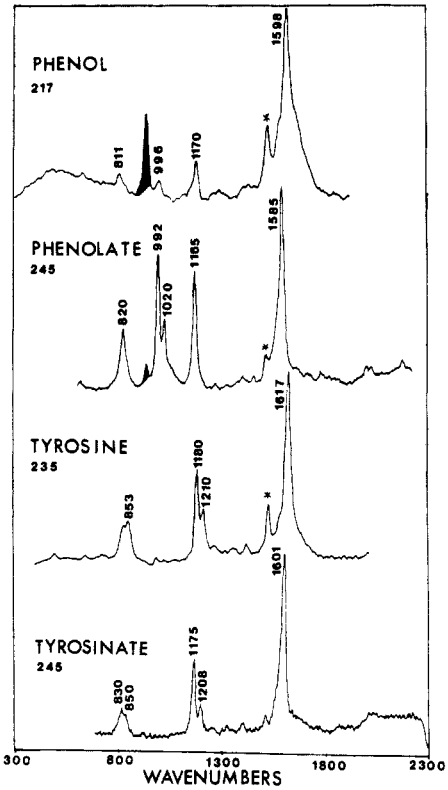

Figure 5. Resonance Raman spectra of aqueous solutions of phenol and related compounds. (A) Phenol (5.0 mM) at pH 7.0. Excitation wavelength = 217 nm. Average power = 10 mW. Spectral resolution = ca. 16 cm^{-1}. (B) Phenolate (5.0 mM) at pH 11.5. Excitation wavelength = 245 nm. Average power = 3 mW. Spectral resolution = ca. 12 cm^{-1}. (C) Tyrosine (5.0 mM) at pH 7.0. Excitation wavelength = 235 nm. Average power = 16 mW. Spectral resolution = ca. 14 cm^{-1}. (D) Tyrosinate (5.0 mM) at pH 11.5. Excitation wavelength = 245 nm. Average power = 3 mW. Spectral resolution = ca. 12 cm^{-1}. The shaded peak at 932 cm^{-1} derives from the sodium perchlorate internal intensity standard. Peaks labeled with * are due to a photochemical transient[6,27] (see text for details).

Table III. Assignments and Depolarization Ratios of the Raman Bands of the Aromatic Amino Acids[a,b]

frequency, cm^{-1}	assignment	description	ρ
		phenylalanine[c]	
		I. Fundamentals	
790	ν_1	symmetric ring breathing	
1006	ν_{12}	symmetric ring stretch (b_{1u})	
1030	ν_{18a}	in-plane CH bend	
1182	ν_{9a}	in-plane CH bend	
1207	ν_{7a}	phenyl–C stretch	
1593	ν_{8b}	in-plane ring stretching	
1604	ν_{8a}	in-plane ring stretching	
		II. Combinations and Overtones	
2005	$2\nu_{12}$		
2193	$\nu_{12} + \nu_{9a}$		
2365	$2\nu_{9a}$		
2579	$\nu_{12} + \nu_{8a}$?		
2757	$\nu_{9a} + \nu_{8a}$		
		tyrosinate[d]	
		I. Fundamentals	
830	$2\nu_{16a}$	Fermi resonance doublet	0.6 ± 0.4
850	$+ \nu_1$	symmetric ring stretch	
1175	ν_{9a}	in-plane CH bend, C_6H_5–C stretch	0.39 ± 0.15
1208	$\nu(a_1)$	totally symmetric stretch	
1270	ν_{7a}	20% C–O stretching and symmetric ring deformation	
1556	ν_{8b}	in-plane ring streching	
1601	ν_{8a}	in-plane ring stretching	0.37 ± 0.09
		II. Combinations and Overtones	
2038	1208 + 830, 1175 + 850		
2337	$2\nu_{9a}$		
2426	ν_{8a} + 850, 830		
2784	$\nu_{9a} + \nu_{8a}$		
2894	$\nu_{7a} + \nu_{8a}$		
		tryptophan[e]	
		I. Fundamentals	
757		symmetric benzene/pyrrole in-phase breathing vibration	0.26 ± 0.04
877	ν_{10a}	indole ring vibration with NH bending	
1006		symmetric benzene/pyrrole out-of-phase breathing vibration	0.30 ± 0.04
1232			0.33 ± 0.20
1350		pyrrole ring vibration	0.38 ± 0.05
1460			0.4 ± 0.1
1550	ν_{8a}	symmetric phenyl ring mode	0.35 ± 0.05
1578		pyrrole vibration	
1614	ν_{8b}	phenyl ring vibration	<1.00[f]
		II. Combinations and Overtones	
1768	1006 + 757		
1887	757 + 1134		
1995	757 + 1232		
2015	2(1006)		
2125	877 + 1232		
2325	877 + 1460		
2579	1232 + 1350		
2800	1232 + 1550 or 1350 + 1460		

[a] Benzene mode numbering from Table II and ref 38. [b] Depolarization ratios measured at 235-nm excitation. [c] Assignments derive from ref 36c. [d] Assignments derive from ref 36, 41f [e] Assignments derive from ref 39a and 39b. [f] Because of overlap we can only give an upper bound.

and selected depolarization ratios for phenylalanine and other aromatic amino acids.

Figure 4B shows the resonance Raman spectrum of tyrosinate measured with 218-nm excitation. The tyrosinate vibrations enhanced in the L_a transition are identical with those enhanced by similar excitation in phenol and phenolate[6] (Figure 5). The unresolved doublet at 830/850 cm^{-1} in tyrosinate which has previously been used to monitor the tyrosine environment in normal Raman protein studies derives from a Fermi resonance between the symmetric ring breathing fundamental (ν_1) and the overtone of the ν_{16} (413 cm^{-1}) ring deformation mode[19,35] (an out-of-plane C–H bend of a_1 symmetry). The band at 1175 cm^{-1} is the ν_{9a} in-plane CH deformation. The 1208-cm^{-1} band is a symmetric ring stretching mode which is commonly observed in para-substituted benzene derivatives (compare Figure 5). The band at 1270 cm^{-1} (ν_{7a}) which derives from a symmetric ring breathing vibration is unique because in phenolate and, presumably, tyrosinate, this vibration has a 20% C–O stretching contribution.[38] This is the only enhanced vibration with a large contribution from C–O stretching. The bands at 1601 and 1556 cm^{-1} derive from the ν_{8a} and ν_{8b} benzene vibrations, respectively. Tyrosinate Raman spectra excited at longer wavelength (235 nm, Figure 4C) show a dramatically decreased enhancement for the 1270-cm^{-1} and the 1556-cm^{-1} peaks.

Resonance Raman spectra of tryptophan excited at 220 and 273 nm are shown in Figure 4D and 4E, respectively. Some of the peak assignments listed in Table III derive from Hirakawa et al.[39a] The intense bands observed with 220-nm excitation at 757 and 1006 cm^{-1} derive from the ν_1 symmetric ring stretch of benzene and the symmetric ring stretch of pyrrole.[39] These modes couple in indole to produce the 757-cm^{-1} (1006-cm^{-1}) peak when they couple in-phase (out-of-phase). The 877-cm^{-1} band is an in-plane indole vibration with a contribution from NH in-plane deformation. The band at 1350 cm^{-1} which derives mainly from a pyrrole ring vibration is known to be sensitive to local environment.[23,24,39] The band at 1550 cm^{-1} is a symmetric stretching mode (ν_{8a}, vide infra) of the indole ring similar to that observed in naphthalene.[39a] The bands at 1578 and 1614 cm^{-1} are in-plane ring vibrations and derive from a pyrrole vibration and the ν_{8b} mode of benzene, respectively. The 1578-cm^{-1} vibration is the most intense feature upon excitation at 273 nm in resonance with the tryptophan L_a, L_b transitions. Peak assignments for the resonance enhanced bands of tryptophan are tabulated in Table III.

The total differential Raman cross-section excitation profiles and the absorption spectrum of phenylalanine are shown in Figure 6. The Raman cross sections increase dramatically as the excitation frequency approaches the L_a absorption band maximum at ca. 205 nm. As previously observed for benzene, little enhancement occurs for resonance with the L_b transition.[2] Maximal phenylalanine enhancement is expected to occur further in the UV. This expectation is confirmed in the recent 200- and 218-nm excited spectra of Rava and Spiro,[21] however; in contrast to Rava and Spiro's results for 240- and 218-nm excitation, our excitation profiles for the 1006- and 1604-cm^{-1} bands show a smooth intensity increase between 240 and 218 nm. Possibly, the discrepancy derives from an increased Raman intensity from their 3400-cm^{-1} water internal intensity standard peak. With ca. 220-nm excitation, the 1604-cm^{-1} ν_{8a} mode dominates the Raman spectra. The 750- (not shown), 1006-, 1030-, 1182-, and 1207-cm^{-1} bands also show preresonance enhancement as the L_a transition is approached. We were unable to accurately determine the 750-cm^{-1} mode excitation profile because it is relatively weak and overlaps other modes.

The solid lines drawn through the excitation profile data for the 1604- and 1006-cm^{-1} peaks derive from fits of the data to a modified[2,4] Albrecht *A*-term expression.[40,41] This expression

(38) Pinchas, S. *Spectrochim. Acta Part A* **1972**, *28A*, 801.
(39) (a) Hirakawa, A. Y.; Nishimura, Y.; Tadashi, M.; Nakanishi, M.; Tsuboi, M. *J. Raman Spectrosc.* **1978**, *7*, 282. (b) Lord, R. C.; Miller, R. A. *J. Chem. Phys.* **1942**, *10*, 328.
(40) Tang, J.; Albrecht, A. C. In *Raman Spectroscopy, Theory and Practice*; Szymanski, H. A., Ed.; Plenum: New York, 1970; Vol. II, 33.
(41) Albrecht, A. C.; Hutley, M. C. *J. Chem. Phys.* **1971**, *55*, 4438.

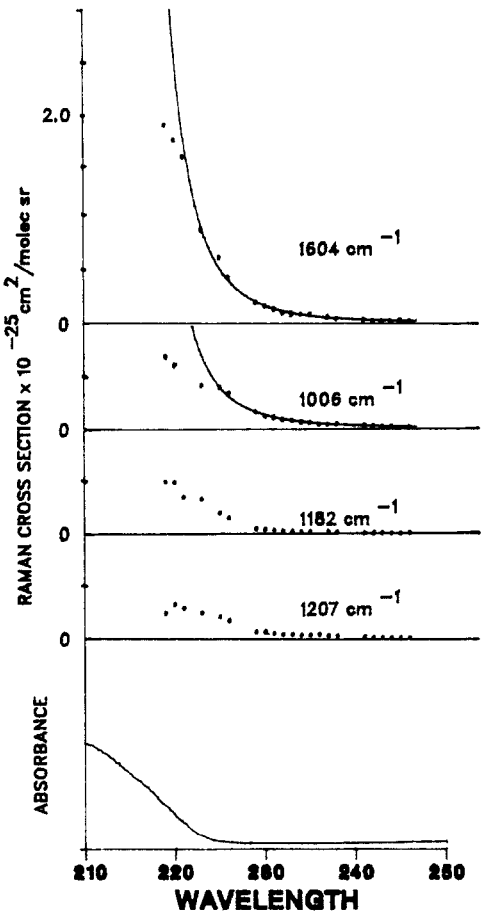

Figure 6. Phenylalanine absorption spectrum and the total differential Raman cross-section excitation profiles. Because of the overlap between the 1182- and 1207-cm^{-1} peaks, these excitation profiles should only be considered as semiquantitative monitors of the wavelength dependence of the cross sections. The curves through the 1604- and 1006-cm^{-1} data derive from an A-term preresonance fit of the data. See text for details.

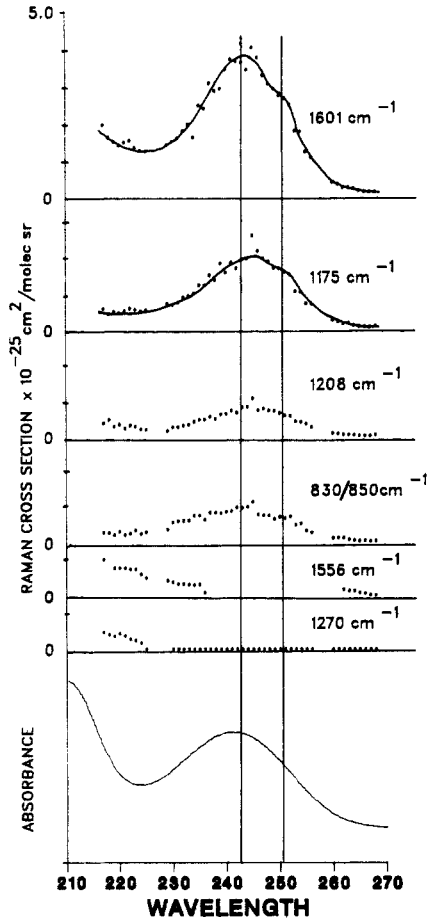

Figure 7. Tyrosinate absorption spectrum and total differential Raman cross-section excitation profiles. The excitation profile of the 1556-cm^{-1} peak is not shown between 235 and 260 nm because of spectral overlap with the intense 1601-cm^{-1} peak. The lines through the points are to aid the eye of the reader. The data relative standard deviation derives mainly from errors in estimates of the spectral background. We estimate that the relative standard deviation is 10%.

effectively models preresonance enhancement if excitation occurs relatively far from resonance and if enhancement is dominated by a single electronic transition. All but the three shortest wavelength excitation profile data were utilized in the fit. The decrease in the slope at the shortest wavelengths suggests that we are too far into resonance to apply the A-term expression to these data points. It should be noted that 200-nm excitation[21b] increases the relative intensity of the 1006-cm^{-1} band. Presumably, this is related to the fact that 200-nm excitation occurs between the L_a and $B_{a,b}$ transitions.

The modified A-term models the preresonant enhancement as if it derives from one isolated electronic transition at higher energy and one other state in the far UV (vide infra). The electronic transition giving rise to the intensity increase evident in Figure 6 is extrapolated to occur at ca. 210 nm for both the 1006- and 1604-cm^{-1} peaks. The absorption maximum of the L_a transition occurs at ca. 205 nm, while the λ_{max} of the first allowed $B_{a,b}$ transition occurs at ca. 190 nm. The A-term fits indicate that the L_a transition is the dominant source of preresonance enhancement for both of these vibrations. This behavior is distinctly different than in benzene where the preresonant state was extrapolated[2] to occur at 191 nm. For benzene the E_{1u} state ($B_{a,b}$) dominates the ν_1 preresonance enhancement.

The absorption spectrum and the excitation profiles of tyrosinate are shown in Figure 7. The excitation profile maxima of most Raman bands occur on the long wavelength side of the 240-nm L_a absorption band maximum. The maxima for the 830/850-cm^{-1} doublet and the 1175-, 1208-, and 1601-cm^{-1} modes of tyrosinate occur at ca. 245 nm. The 1601-cm^{-1} ν_{8a} mode dominates the Raman spectrum for excitation within the L_a transition. This same mode dominates the Raman spectra of toluene and phenylalanine for excitation close to the L_a absorption band. Most of the tyrosinate bands shown in Figure 7 are resonance enhanced by the L_a transition. These include both the ν_{8a} band and the ν_{9a} 1175-cm^{-1} band, which in phenylalanine (1182 cm^{-1} for ν_{9a}) shows strong preresonance enhancement by the L_a transition. In contrast, the 1270- (ν_{7a}) and 1556-cm^{-1} (ν_{8b}) bands of tyrosinate show little or no enhancement by the L_a transition but are enhanced primarily by a transition further in the UV.

The absorption spectrum and excitation profiles of tryptophan are shown in Figure 8. Saturation phenomena were observed for excitation close to the tryptophan absorption maxima.[27] The saturation phenomena will cause any vibronic fine structure to become more diffuse and less distinguishable. The measured cross sections for tryptophan must be considered as lower limits.[27] As in tyrosinate, and possibly in phenylalanine, the maximal enhancement of each mode occurs at a wavelength somewhat redshifted from the absorption spectral maximum at 220 nm. The 1006-, 1550-, and 757-cm^{-1} bands are the most intense features upon excitation in resonance with the allowed 220-nm transition. The excitation profiles of the 757-, 877-, 1006-, 1232-, 1350-, 1550-, and 1614-cm^{-1} modes are centered at ca. 223 nm. The 1578-cm^{-1} band of tryptophan, which is not visibly enhanced by the allowed transition at 220 nm, is selectively enhanced by the 270–300-nm absorption band. The 1578-cm^{-1} peak dominates spectra excited in resonance with the overlapping L_a and L_b transitions between 270 and 300 nm.

Table III lists depolarization ratios of peaks observed in the Raman spectra of tyrosinate and tryptophan for excitation at 235 nm. The depolarization ratios of the 1175- and 1601-cm^{-1} peaks of tyrosinate at 235-nm excitation are close to 0.33. The depo-

Table IV. Total Differential Raman Cross Sections of Aromatic Amino Acids[a]

Raman band, cm^{-1}	excitation wavelength, nm						
	220	230	240	250	260	279	488[b]
			Phenylalanine				
1006	0.61	0.129	0.036				2.05
1030	0.29	0.044	0.009				0.47
1182	0.49	0.041	0.007				0.12
1207	0.33	0.069	0.015				0.34
1604	1.76	0.170	0.037				0.38
			Tyrosinate				
830/850	0.32	0.56	0.85	0.70	0.14		0.68/0.54
1175	0.48	0.70	1.6	1.70	0.28		0.38
1208	0.36	0.28	0.64	0.65	0.11		0.64
1270	0.42	0.09					0.40
1556	0.77	0.39					
1601	1.41	1.51	3.50	2.75	0.44		1.34
			Tryptophan[c]				
757	9.2	4.7	0.49	0.11	0.50	0.07	1.3
877	1.5	0.62	0.05	0.00	0.00	0.00	0.35
1006	8.3	3.8	0.40	0.10	0.05	0.02	1.56
1232	1.6	0.43	0.05	0.00	0.02	0.04	
1350	3.6	1.3	0.30	0.13	0.08	0.13	1.01
1460	0.6	0.22	0.11	0.06	0.06	0.07	0.67
1550	6.4	2.10	0.41	0.12	0.10	0.15	1.35
1578	*d*	*d*		0.08	0.16	0.35	0.50
1614	1.3	0.80	0.43	0.30	0.26	0.21	0.34

[a] Cross section units are 10^{-25} $cm^2/(molecule\ sr)$. [b] Cross section units are 10^{-29} $cm^2/(molecule\ sr)$. [c] Cross sections values are lower limits. [d] Strongly overlapped by adjacent peaks.

larization ratios at 235-nm excitation of the 1006-, 1232-, 1350-, 1460-, 1550-, and 1614-cm^{-1} modes of tryptophan are ca. 0.33, while the depolarization ratio of the 757-cm^{-1} mode is slightly less. Thus, all strongly enhanced vibrations of tyrosinate, phenylalanine, and tryptophan are polarized and symmetric.

Depolarization ratios of 0.33 are indicative of the predominance of one diagonal tensor element if the dominant enhancement mechanism is *A*-term Franck–Condon scattering. Thus, the observation of depolarization ratios close to 0.33 indicates that the resonant transition, which dominates the Raman intensities, is not degenerate and is linearly polarized. In contrast, the depolarization ratios of the 757-cm^{-1} band of tryptophan appear to differ from 0.33 and suggest the contribution of additional tensor elements. This could indicate the presence of additional resonant states, overlap with another Raman peak, and/or additional scattering mechanisms.

Table IV lists the measured absolute Raman cross sections of some of the modes of tryptophan, tyrosinate, and phenylalanine. The cross-section values for tryptophan as displayed in the excitation profiles are, as indicated above, lower limits.

Discussion

The selective resonance enhancement of particular vibrations and the Raman excitation profile data can be understood by considering the factors important for Raman intensity. The total Raman scattering cross section, σ_{mn}, for the Raman vibrational transition $n \leftarrow m$ over 4π sr for an isolated molecule averaged over all orientations is[3,40-44] as in eq 1. I_{mn} is the integrated Raman

$$\sigma_{mn} = \frac{I_{mn}}{I_0} = \frac{2^7\pi^5}{3^2}\nu_0(\nu_0 - \nu_{mn})^3 GF(T)|\sum_{\rho\sigma}\alpha_{\rho\sigma}(\nu_0)|^2 \qquad (1)$$

scattered intensity (photons/(s cm^2)) over 4π sr integrated over the bandwidth of the vibrational transition $n \leftarrow m$. I_0 and ν_0 are the incident excitation beam intensity and frequency (cm^{-1}), while ν_{mn} corresponds to the frequency of the Raman vibrational mode (cm^{-1}). G is a factor specifying the degeneracy of the initial state, m, while $F(T)$ is the Boltzmann weighting factor specifying the thermal occupancy of the initial state. The factor $\nu_0(\nu_0 - \nu_{mn})^3$ appears rather than $(\nu_0 - \nu_{mn})^4$ (as is commonly seen) because the intensities are defined in units of photons/(s cm^2) for photon

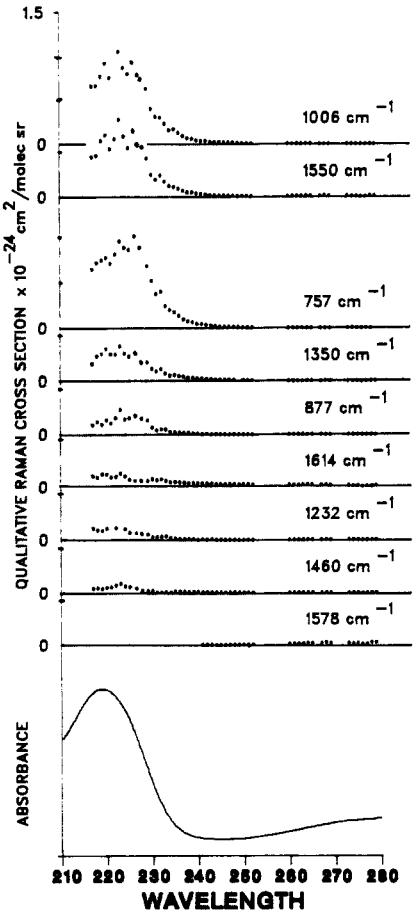

Figure 8. Tryptophan absorption spectrum and qualitative Raman excitation profiles. The excitation profile data suffer from optical saturation phenomena, and the cross sections shown are lower bounds. See text for details.

(42) Schrotter, H. W.; Klochner, H. W. In *Topics in Current Physics*; Weber, A., Ed.; Springer-Verlag: Berlin, 1979; p 123.
(43) Eckhardt, G.; Wagner, W. G. *J. Mol. Spectrosc.* **1977**, *6*, 38.
(44) Mortensen, O. S.; Hassing, S. In *Advances in Infrared and Raman Spectroscopy*; Clark, R. J. H., Hester, R. E., Eds.; Heyden: London, 1980; Vol. 6, p 1.

counting detection. $\alpha_{\rho\sigma}(\nu_0)$ is the ρ, σth ($\rho, \sigma = x, y, z$) component of the Raman polarizability tensor averaged over all molecular orientations for the excitation frequency, ν_0.

For 90° Raman scattering measurements from a solution where the incident light is polarized perpendicular to the scattering plane, and both the parallel and perpendicular scattering polarization are collected, the total differential Raman scattering cross section, σ_R, is given by[3,42-46]

$$\sigma_R = \frac{d\sigma_{mn}(\nu_0)}{d\Omega} = \frac{2^4\pi^4}{45} b^2 G \frac{L\nu_0(\nu_0 - \nu_{mn})^3}{1 - \exp(-hc\nu_{mn}/kT)}(45\alpha^2 + 7\gamma^2 + 5\delta^2) \quad (2)$$

where b is the zero-point vibrational amplitude

$$b = (h/8\pi c^2 \nu_{mn})^{1/2}$$

α^2, γ^2, and δ^2 are the isotropic, anisotropic, and antisymmetric[46] invariants of the polarizability tensor, and h, c, k, and T are Planck's constant, the speed of light, Boltzmann's constant, and the temperature, respectively. L is the local field correction for the condensed-phase sample and specifies the increased electric field amplitude in the sample over that which would be present in the gas phase.[42,47]

The components of the polarizability tensor, $\sigma_{\rho\sigma}$, are given by second-order perturbation theory as[40,48] in eq 3 where ρ and σ are molecular coordinates which label the components of the polarizability tensor. R_σ is the electric dipole moment operator along

$$\alpha_{\rho\sigma} = \sum_{ev} \frac{\langle gm|R_\sigma|ev\rangle\langle ev|R_\rho|gn\rangle}{\nu_{ev} - \nu_m - \nu_0 - i\Gamma e} + \frac{\langle gm|R_\rho|ev\rangle\langle ev|R_\sigma|gn\rangle}{\nu_{ev} - \nu_n + \nu_0 + i\Gamma e} \quad (3)$$

the molecular coordinate, σ. ν_{ev} is the transition frequency from the ground state to the v vibrational level of the excited electronic state, e. Γ_e is the excited state line width. The summation in eq 3 is over all molecular excited states ev except for the ground state. The Raman transition occurs between vibrational levels m and n of the ground electronic state, g.

This expression predicts that the Raman intensity will increase as resonance is approached. In normal Raman scattering, numerous electronic transitions contribute to the Raman intensity; the contribution of each transition is weighted by the magnitude of the transition moments in the numerator as well as the energy terms in the denominator. Given similar transition moments, the electronic transition closest to the excitation frequency should contribute most.

The expression for the Raman polarizability can be separated into three terms which describe three different enhancement mechanisms.

$$\alpha_{\rho\sigma} = A + B + C$$

In the case of a symmetric vibration enhanced by an allowed electronic transition, the major source of enhancement derives from the A term in which the scattered intensity results from Franck–Condon overlap factors (eq 4).

$$A = [\langle g|R_\sigma|e\rangle\langle e|R_\rho|g\rangle]\sum_v \frac{\langle m|v\rangle\langle v|n\rangle}{\nu_{ev} - \nu_m - \nu_0 - i\Gamma_e} \quad (4)$$

For nontotally symmetric vibrations, non-Condon contributions to enhancement occur through Herzberg–Teller coupling between different excited electronic states e and s through the B term where h_a is the vibronic coupling operator for the normal mode of interest. Modes which vibronically borrow intensity from allowed transitions will be enhanced by the B term.

$$B = 2\sum_{e\neq gs\neq e}\sum \frac{\langle g|R_\sigma|e\rangle\langle e|h_a|s\rangle\langle s|R_\rho|g\rangle}{\nu_e - \nu_m - \nu_0 - i\Gamma_e} \frac{\langle m|Q_a|n\rangle}{\nu_e - \nu_s} \quad (5)$$

$$h_a = (\partial H_e/\partial Q_a)$$

The Albrecht "C" term, describes B-term-like coupling between the ground state and excited states is small, in general, especially for resonance excitation in the UV where the excited- and ground-state energy differences are large compared to the energy differences between excited states. For resonance excitation in dipole forbidden transitions, where $\langle e|R_\rho|g\rangle$ is identically zero, a higher order perturbation expression is required which results in enhancement mainly of overtones and combinations. This term, which is *now* known as the C term, derives purely from vibronically induced oscillator strength in the resonant (or preresonant) transition.[7,8,49] It should be noted that this C term differs from that discussed earlier by Tang and Albrecht.[40]

Since both the resonance- and presonance-enhanced vibrations of the aromatic amino acids are symmetric, we will assume that the enhancement of these modes is dominated by the A term. Symmetric modes can also be enhanced by non-Condon sources such as the B and C terms,[50] but these sources of enhancement are generally much smaller than that from the A term. We also assume that the A-term enhancement derives from a geometric distortion of the excited state relative to the ground state, and we neglect enhancement via alterations in the bond force constants. These assumptions could easily be relaxed without resulting in any changes in the major conclusions.

For preresonance excitation the frequency dependence of the Raman cross section which derives from the modified A term[12,41] is in eq 6. The B term frequency dependence is in eq 7 where ν_e and ν_s are the transition frequencies to the excited electronic states which dominate the preresonance enhancement. K_1 and

$$\sigma_A = K_1\nu_0(\nu_0 - \nu_{mn})^3\left(\frac{\nu_e^2 + \nu_0^2}{(\nu_e^2 - \nu_0^2)^2} + K_2\right)^2 \quad (6)$$

$$\sigma_B = K_3\nu_0(\nu_0 - \nu_{mn})^3\left(\frac{\nu_e\nu_s + \nu_0^2}{(\nu_e^2 - \nu_0^2)(\nu_s^2 - \nu_0^2)}\right)^2 \quad (7)$$

K_3 are scaling factors which are proportional to the matrix elements in the numerators of the A and B terms. K_2 is a term which is utilized to phenomenologically account for the contributions of other excited states, expecially those in the far UV ($\nu_e \rightarrow \infty$). These preresonance expressions are expected to model the data well when the Raman excitation is sufficiently far from resonance that $|\nu_{ev} - \nu_0| \gg \nu_{nm}$.

Phenylalanine. Only totally symmetric vibrations show preresonance enhancement in toluene and phenylalanine. The preresonance A term fits to the excitation profile data for the 1601-cm^{-1} ν_{8a} and the 1006-cm^{-1} ν_{12} vibrations indicate that their preresonance enhancement is dominated by the L_a state and suggest that the L_a transition occurs at ca. 210 nm. The 1182- and 1207-cm^{-1} excitation profiles show curvatures similar to those of the 1006- and 1604-cm^{-1} modes, indicating that they are also preresonance enhanced by the L_a transition. In contrast, the ν_1 vibration (786 cm^{-1} in toluene, 750 cm^{-1} in phenylalanine) shows little preresonance enhancement from the L_a transition. Numerous bands are observed in the toluene and phenylalanine UV Raman spectra. In benzene the only fundamental vibration observed with significant intensity was the ν_1 992-cm^{-1} symmetric ring breathing mode. For benzene the ν_1 vibration is preresonance enhanced[2] primarily by the E_{1u} state at 185 nm.

The spectral differences between benzene and the monosubstituted benzene derivatives, toluene and phenylalanine, result from the decrease in effective symmetry to C_{2v}. The three lowest energy excited states of benzene are of B_{2u}, B_{1u}, and E_{1u} symmetry (Figure

(45) Skinner, J. G.; Nilsen, W. G. *J. Opt. Soc. Am.* **1968**, *58*, 113.
(46) Long, D. A. *Raman Spectroscopy*; McGraw-Hill: New York, 1977.
(47) Abe, N.; Wakayama, M.; Ito, M. *J. Raman Spectrosc.* **1977**, *6*, 38.
(48) Albrecht, A. C. *J. Chem. Phys.* **1961**, *34*, 1476.
(49) (a) Ziegler, L. D.; Albrecht, A. C. *J. Raman Spectrosc.* **1979**, *8*, 73. (b) Ziegler, L. D.; Albrecht, A. C. *J. Chem. Phys.* **1977**, *67*, 2753. (c) Ziegler, L. D.; Albrecht, A. C. *J. Chem. Phys.* **1979**, *70*, 2634, 2644.
(50) Stallard, B. R.; Callis, P. R.; Champion, P. M.; Albrecht, A. C. *J. Chem. Phys.* **1984**, *80*, 70.

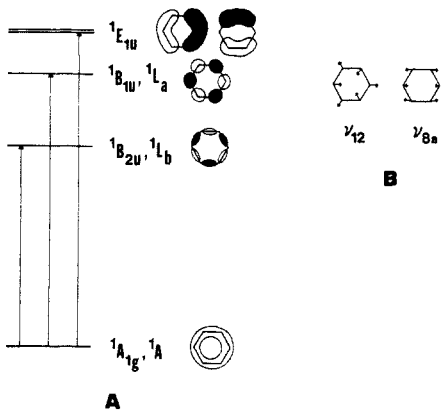

Figure 9. (A) Electronic transitions and the excited states of benzene and its derivatives.[53] (B) Carbon atomic displacement coordinates of the ν_{12} and ν_{8a} vibrations.[36c,54]

9). Electric dipole transitions to the B_{2u} and B_{1u} states are symmetry forbidden, while the transition to the E_{1u} state is allowed. Thus, the benzene absorption spectrum is dominated by the strong 185-nm E_{1u} absorption band. The formally forbidden B_{1u} and B_{2u} transitions at ca. 205 and 250 nm have low but non-zero oscillator strengths because of Herzberg–Teller coupling to the E_{1u} state by e_{2g} vibrations. The vibronic structure evident in the B_{2u} and B_{1u} transitions derives from Franck–Condon progressions in the ν_1 symmetric ring stretch. These progressions are built upon one quantum of the ν_6 e_{2g} Herzberg–Teller mixing mode (521 cm^{-1} in the excited state, 628 cm^{-1} in the ground state). In benzene, essentially no preresonance enhancement is evident for the ν_1 vibration from the B_{1u} and B_{2u} transitions because they are dipole forbidden. Thus, the dominant source of ν_1 enhancement is the 185-nm E_{1u} excited state; however, the apparent 120-nm far UV transition[49b,c] also contributes and dominates Raman intensity for excitation in the visible and near-UV spectral region. No enhancement by the E_{1u} transition was observed in benzene for the other totally symmetric vibration, the ν_2 3073-cm^{-1} C–H stretch, presumably because this vibration negligibly perturbs the $\pi \rightarrow \pi^*$ transitions. Indeed, recent data on gas-phase benzene show that the ν_2 vibration is enhanced only by a transition or transitions centered around 120 nm.[51]

The local ring symmetry of monosubstituted benzene derivatives is C_{2v}. The benzene B_{2u}, B_{1u} excited-state symmetries correlate with symmetries of B_1, A_1 in the C_{2v} point group. The excited states are labeled as L_b and L_a. The E_{1u} transition splits into two allowed transitions to states of A_1 and B_1 symmetry known as the B_a and B_b transitions, respectively. The L_a (B_{1u}) transition is no longer symmetry forbidden and can now act as a source of preresonance enhancement. Substitution of an alkyl group on the ring increases the B_{1u} transition oscillator strength[33b] by ca. 20%. The oscillator strength of the $B_{a,b}$ (E_{1u}) transition also shows a small increase. Thus, the enhancement of the ν_1 vibration of benzene should be similar to that of toluene or phenylalanine, provided the same atomic displacements occur and no dramatic absorption spectral shifts occur. Indeed, this is the behavior observed for toluene and phenylalanine. The cross section of the ν_1 vibration at 220-nm excitation is $15 \pm 3 \times 10^{-27}$ cm^2/(molecule sr) for both benzene[2] and toluene,[52] while it is ca. 10×10^{-27} cm^2/(molecule sr) for phenylalanine.

The dramatic spectral differences between benzene and toluene and phenylalanine occur because the ring substituents lift[8] the degeneracy of the e_{2g} vibrations. The vibrational symmetries in the C_{2v} point group become a_1 and b_1. These a_1 modes can now be enhanced by the Franck–Condon *A*-term mechanism. We estimate from published data[2,7] that the cross section of the ν_8 e_{2g} vibration in benzene is ca. 1×10^{-28} cm^2/(molecule sr) (5×10^{-27} cm^2/(molecule sr)) for excitation at 220 nm (212.8 nm). For phenylalanine (toluene) the cross section is 1.8×10^{-25} cm^2/(molecule sr) (0.8×10^{-25} cm^2/(molecule sr)) for excitation at 220 nm. Thus, at 220 nm the cross sections of the toluene and phenylalanine ν_{8a} vibrations increase by factors of ca. 1000 compared to the ν_8 benzene vibration. This huge intensity increase occurs in conjunction with only small spectral shifts and oscillator strength increases in the absorption spectra. The dominance of *A*-term enhancement is strongly supported by the satisfactory fits of the Figure 6 excitation profiles to an *A*-term expression with a 210-nm transition. Any *B*-term enhancement would presumably result from vibrational coupling between the L_a state and the strongly allowed $B_{a,b}$ states. Any preresonance *B*-term fit would show less curvature than that shown in Figure 6.

To emphasize, these vibrations are enhanced because they are *now* of a_1 symmetry. Their *A*-term activity occurs in preresonance with the L_a transition which possesses oscillator strength due to vibronic coupling with the $B_{a,b}$ state and because of the symmetry reduction caused by the ring substituent.

For monosubstituted benzenes, all of the enhanced vibrations are of a_1 symmetry except for the ν_{8b} vibration which appears as a shoulder at 1593 cm^{-1} in the 220-nm excited phenylalanine spectrum and is well resolved in the phenylalanine spectra[21] excited at 218 and 200 nm. There are a total of 30 fundamental vibrations in monosubstituted benzene derivatives, of which 24 are essentially independent of the ring substituent. The six vibrations whose frequencies show a strong dependence on the nature of the substituent have significant contributions from ring carbon–substituent carbon stretching.[36c] All of these vibrations can be Raman active, at least as far as symmetry selection rules. Eleven of these vibrations are of a_1 symmetry, and six of these, the ν_1, ν_{12}, ν_{18a}, ν_{9a}, ν_{7a}, and ν_{8a} vibrations are resonance enhanced. In toluene and phenylalanine, all but the ν_1 vibration appear to derive their preresonance intensity enhancement from the L_a transition.

The selection of these five vibrations for preresonance enhancement by the L_a transition occurs because of the atomic displacements active in the vibration. The enhancement of the ν_{12} vibration occurs because of the trigonal nature of the carbon displacements which occurs during the vibration (Figure 9). In benzene this vibration was of b_{1u} symmetry. The transition electron density (the change in electron density between the excited and ground states[53]) has the same symmetry as that of the phasing of the wave function of the excited state shown in Figure 9. A distortion of the ground state by a b_{1u} symmetry vibration would distort the ground-state electron density (and presumably geometry) toward a configuration similar to that of the B_{1u}-like L_a phenylalanine and toluene excited states. Both the excited state and ground state are of A_1 symmetry in the C_{2v} point group. Thus, the ν_{12} mode is strongly Franck–Condon *A*-term-active because it distorts the molecule toward the excited-state configuration. The other b_{1u} mode, ν_3 at ca. 3060 cm^{-1} is not enhanced because C–H stretching does not significantly change the π-electron density.

The ν_{8a} vibration is resonance enhanced for the same reason as the ν_{12}: this vibration in monosubstituted derivatives has a trigonal nature to its atomic displacements. Every other atom moves in an opposite direction with respect to planes through the center of the ring. This results in displacements of the ground-state geometry in a monosubstituted benzene derivative which will increase or decrease the charge density with a pseudosymmetry similar to that of B_{1u} in the D_{6h} point group. The ν_{9a}, ν_{7a}, and ν_{18a} vibrations also have some trigonal distortion characteristics in their atomic displacement coordinates. The other a_1 vibrations either do not show a trigonal displacement pattern or they involve C–H ring stretches which do not significantly affect the π orbital electron density or the carbon framework molecular ground-state geometry.

The relative contribution of the L_a state to the preresonance enhancement can be monitored by comparing the values of the

(51) Harmon, P. A.; Johnson, C. R.; Asher, S. A. to be submitted for publication in *J. Chem. Phys.*

(52) Johnson, C. R.; Asher, S. A. to be submitted for publication in *J. Phys. Chem.*

(53) Salem, L. *The Molecular Obital Theory of Conjugated Systems*; Benjamin: New York, 1966.

preresonance and K_2 term at a particular excitation wavelength (eq 6). For the 1604-cm^{-1} vibration at 220-nm (230-nm) excitation, the L_a preresonance term contributes 75 (20) times that of K_2. For the 1006-cm^{-1} vibration for 220-nm (230-nm) excitation, the L_a preresonance term contributes 18 (5) times that of K_2. Thus, the L_a state dominates the UV intensities. For visible wavelength excitation at 488 nm, the constant term (K_2) dominates. The relative L_a state contribution to the Raman intensities compared to the far-UV state (K_2 term) is 0.13 and 0.55 for the 1006- and 1604-cm^{-1} vibrations, respectively. Thus, the L_a state contribution for visible wavelength Raman intensities is small, especially for the 1006-cm^{-1} peak. This behavior is similar to that observed for the ν_1 band of benzene.[2]

Tyrosinate. The vibrational modes enhanced with UV excitation in tyrosinate are essentially identical with those in phenylalanine. Para-substituted derivatives are formally of C_{2v} symmetry, but if the substituents are similar the molecular symmetry approximates D_{2h}.[54] Modes of gerade symmetry are Raman allowed. The ν_1 vibration is enhanced as part of the 830/850-cm^{-1} Fermi doublet. A symmetric mode around 1000 cm^{-1} analogous to the ν_{12} mode of monosubstituted derivatives does not exist for para-substituted benzenes. Strongly enhanced ν_{9a} and ν_{8a} modes of a_{1g} (D_{2h}) or a_1 (C_{2v}) symmetry occur at 1175 (1180 cm^{-1}) and 1601 cm^{-1} (1617 cm^{-1}) in tyrosinate (tyrosine). The ca. 1210-cm^{-1} mode derives from an a_1 vibration of para-substituted benzene. The 1270-cm^{-1} peak derives from a vibration which has a large C–O stretching contribution, as evident from isotopic substitution studies.[38]

It is likely that the 1270-cm^{-1} band derives from the ν_{14} vibration of para-substituted benzenes. This vibration is of b_{2u} symmetry in the D_{6h} or D_{2h} point groups. For similar para ring substituents, the approximate benzene ring symmetry is D_{2h} and the b_{2u} vibration is not Raman allowed. For cases where the para substituents are very different, the appropriate point group is C_{2v} and this vibration becomes Raman allowed. Excitation further into the UV may result in charge-transfer excitations, which may intimately involve the OH group[53,55] (vide infra) and result in a decrease in the effective molecular symmetry due to an induced inequivalence of the para substituents. This will increase the allowedness of this vibration. The presence of charge-transfer character in far-UV states may account for the increasing 1270-cm^{-1} intensity for far-UV excitation. As in toluene, phenol, and phenylalanine, the ν_{8b} vibration is the only nontotally symmetric vibration enhanced.

The excitation profiles shown in Figure 8 demonstrate that the tyrosinate L_a transition enhances all but the 1556-cm^{-1} ν_{8b} and the 1270-cm^{-1} vibrations. The large enhancement of the ν_{8a} band and its proximity to the ν_{8b} band make it impossible to determine the magnitude of enhancement of the ν_{8b} vibration in the L_a transition. The 1270-cm^{-1} band intensity shows no L_a enhancement within experimental error.

We were unable to excite within the tyrosinate L_b transition because of the onset of fluorescence at excitations of $\lambda > 269$ nm, but 279-nm excited spectra of the dipeptide glycyl tyrosinate at pH 12.8 indicate that the 1270-cm^{-1} C–O stretch, the 830/850-cm^{-1} Fermi resonance doublet, and the ν_{8b} vibration are enhanced by the L_b transition. The tyrosinate fluorescence is partially quenched in the dipeptide. For 279-nm excitation, the intensities of the 830/850-cm^{-1} doublet and the 1270-cm^{-1} ν_{8b} vibrations are about half that of the ν_{8a} vibration. The dipeptide data indicate that the ν_{8a}, ν_{9a}, and 1208 cm^{-1} symmetric stretches are not strongly enhanced by the L_b transition.

The ν_1, ν_{7a}, and ν_{8a} bands are known to be active in the gas-phase fluorescence spectrum of phenol.[57,58] The increased absorbance of the L_b band of tyrosinate compared to that of benzene, toluene, and phenylalanine should result in an increased enhancement of symmetric vibrations.

Excitation within the L_a band results in strong enhancement for a_1 vibrations. The ca. 245-nm excitation profile maxima are red shifted 5 nm from the absorption spectral maximum. The shoulder in the excitation profile at 252 nm presumably indicates the position of the O–O transition of the tyrosinate L_a transition. The 243-nm maximum of the 1601-cm^{-1} excitation profile occurs ca. 1500 cm^{-1} above that of the shoulder and indicates the 0–1 Franck–Condon transition. The 1175-cm^{-1} excitation profile appears to be slightly shifted to longer wavelength (ca. 245 nm, 1200 cm^{-1} from the O–O shoulder), possibly indicating the presence of the 0–1 component of the 1175-cm^{-1} peak. The signal-to-noise ratios of other excitation profiles are insufficient to resolve underlying vibronic structure.

The excitation profile data for the 830/850-cm^{-1} doublet represent an average for these two unresolved peaks. Although the resolution of the spectra was insufficient to determine their individual intensities, the band shapes indicate that no gross alterations of relative intensities occur in the wavelength region studied. This indicates that the 830- and 850-cm^{-1} excitation profiles are relatively similar. This is an important observation because the relative intensity of this doublet monitors (at least in nonresonance Raman) the degree of hydrogen bonding of the phenolic hydroxyl of tyrosine residues. This doublet could be an important UV resonance Raman protein structural probe for tyrosine environment if the relative intensities stay reasonably constant for different excitation wavelengths.

Our observations that the relative intensities are relatively independent of excitation wavelength contrast sharply with those of Rava and Spiro[21] and our previous suggestion.[19] The dramatic alterations in the relative intensities previously observed result from the formation of transient photoionization products by the high power density laser pulse.[6] If sufficient tyrosinate photoproduct is generated, new Raman bands will appear at 810, 975, 1160, 1402, 1510, and 1565 cm^{-1}. The starred peaks in the phenol, phenolate, tyrosine, and tyrosinate spectra at ca. 1510 cm^{-1} in Figure 5 derive from this transient. The overlap of the 810-cm^{-1} peak[6] with the 830/850-cm^{-1} doublet results in an apparent intensity increase for the 830-cm^{-1} component in the 240-nm excited spectra of Rava and Spiro.[21] The 1160-, 1402-, and 1565-cm^{-1} peaks are not evident because they overlap bands already present in tyrosine and tyrosinate. A new band at ca. 1510 cm^{-1} clearly signals formation of the photochemical transient. This peak was incorrectly identified as the ν_{19a} vibration, while the ca. 1400–1410-cm^{-1} peak was incorrectly identified as the ν_{19b} vibration.[21] The 200-nm excited tyrosinate spectrum of Rava and Spiro does indicate a change in the relative intensity of the doublet. No accompanying peaks appear to indicate formation of the photo-transient species; however, the excitation profile behavior of the phototransient species is unknown. The effective quantum yield and the detectability of the photochemical transient are independent functions of excitation wavelength.

The 1270-cm^{-1} excitation profile data can be utilized to examine the charge-transfer character of the tyrosinate and tyrosine electronic transitions. The amount of charge-transfer character in the electronic transitions of para monosubstituted and para disubstituted benzene derivatives has been extensively studied both experimentally and theoretically.[55,57,58] The theoretical and experimental results have not always agreed. The magnitude of enhancement of the phenyl–oxygen stretching vibration (1270 cm^{-1}, ν_{7a}) will correlate with the amount of charge transfer in the transition, if enhancement occurs because of A-term Franck–Condon overlap factors or because the excited-state vibrational frequency changes compared to the ground state.[58] The more charge-transfer character, the greater the electron density change for the phenyl–oxygen bond and the larger the change in the bond force constant. The lack of enhancement of the 1270-cm^{-1} ν_{7a}

(54) Colthup, N. B.; Daly, L. H.; Wiberley, S. E. *Introduction to Infrared and Raman Spectroscopy*; Academic: New York, 1975.
(55) Seliskar, C. J.; Khalil, O. S.; McGlynn, S. P. In *Excited States*; Lim, E. C., Ed; Academic: New York, 1974; p 231.
(56) Ludwig, M.; Asher, S. A. to be submitted for publication in *Biochemistry*.
(57) Carsey, T. P.; Findley, G. L.; McGlynn, S. P. *J. Am. Chem. Soc.* **1979**, *101*, 4502.
(58) Bist, H. D.; Brand, J. C. D.; Williams, D. R. *J. Mol. Spectrosc.* **1966**, *21*, 76.

stretch in the phenolate L_a transition, and the observed enhancement in the L_b state correlate well with the perturbation in the oscillator strengths of the transitions between toluene, phenol, and phenolate, tyrosine, and tyrosinate.[30,32,33b,57] The hydroxyl substituent in these derivatives red shift the L_a and L_b absorption bands compared to toluene or *p*-xylene. The molar absorptivity of the L_a transition remains about the same between derivatives such as toluene and phenol, while the L_b state molar absorptivity increases almost by an order of magnitude. Ionization of tyrosine is accompanied by a 20% increase in the L_a band molar absorptivity while that of the L_b band increases by 60%. Thus, the absorption spectrum suggests that the phenolic substituent selectively perturbs the L_b transition. The lack of enhancement of the ν_{7a} phenyl–oxygen stretch in the L_a transition and its enhancement in the L_b transition is consistent with these expectations. Indeed, fluorescence spectra of gas-phase phenol[58] indicate a 12-cm^{-1} frequency increase for the ν_{7a} vibration in the L_b excited state. The selective intensity increase in the ν_{7a} band at $\lambda < 220$ nm is indicative for significant charge-transfer character in the $B_{a,b}$ states. This expectation is borne out by the 200-nm excited Raman spectrum which show an intense ν_{7a} peak.[21]

The excitation profile data for tyrosinate appear free of photochemical and optical saturation phenomena. This is the first (to our knowledge) complete Raman cross-section excitation profile throughout a single electronic transition in a small molecule. We are in the process of quantitatively analyzing these data in the context of normal mode composition and the ground- and excited-state potential surfaces and transition moments.

Tryptophan. The UV absorption spectrum of tryptophan shows four strong bands which are assigned by using the Platt nomenclature[33b] in a fashion similar to that for benzene. The 280-nm absorption band is thought to contain the $L_a \leftarrow A_1$, $L_b \leftarrow A_1$ transitions[32,59] which appear to be polarized at ca. 60–70° to the long axis. The strong $B_{a,b} \leftarrow A$ absorption band at ca. 220 nm is polarized almost directly along the long axis of the molecule. Both of these absorption bands have oscillator strengths indicative of fully allowed transitions.

The excitation profiles of tryptophan are only semiquantitative because of saturation phenomena which cause an artifactual decrease in the Raman intensities in regions of high absorption, especially for transitions which do not quickly ($<10^{-9}$ s) relax to the ground states. Thus, the true excitation profile cross sections are larger. This saturation will also cause vibronic fine structure to become less pronounced, and the signal-to-noise ratio of the excitation profile will decrease as the relative intensity of the analyte internal standard becomes a function of laser power, beam shape, and focusing. Thus, the structure present in the data of Figure 8 is probably not significant. The saturation phenomena, however, do not affect the relative intensities of the analyte Raman bands, provided no new species are detected.

All of the modes enhanced, except for the 757-cm^{-1} mode, have depolarization ratios at 235-nm excitation of 0.33 within experimental error. This value indicates that these modes are totally symmetric and are enhanced by a linearly polarized transition. For these modes, only one of the diagonal tensor elements differ from zero. The smaller depolarization ratio (0.26) for the 757-cm^{-1} band appears to indicate a small contribution from an additional tensor element or, more probably, the overlap with another weak peak which is more polarized. The two strongest bands at 757 and 1006 cm^{-1} have almost identical excitation profiles because they have extraordinarily similar atomic displacement coordinates. The 757- and 1006-cm^{-1} vibrations result from symmetric and antisymmetric combinations of the symmetric benzene and pyrrole ring breathing motions. The 1550-cm^{-1} band derives from the ν_{8a} vibration of substituted benzene derivatives, while the 1350-cm^{-1} mode is a pyrrole ring vibration.

The cross section of the 1006-cm^{-1} vibration increases by at least a factor of 330 between 279 (3×10^{-27} cm^2/(molecule sr)) and 223 nm (1×10^{-24} cm^2/(molecule sr)). The cross section for the 1006-cm^{-1} band with 488-nm excitation is 1.6×10^{-29}. Thus, a mimimum 10^5-fold enhancement occurs for 220-nm excitation compared to 488-nm excitation.

The factor of 330 enhancement for excitation in the $B_{a,b}$ band at 223 nm compared to excitation in the L_a, L_b band at 279 nm occurs because the oscillator strengths differ by a factor of ca. 10. *A*-term enhancement would result in a ca. 100-fold enhancement, while the ν^4 factor gives an additional factor of 2.3. Thus, a relative intensity increase of 200–300 is expected. We, however, are not certain of the cross-section values in the L_a, L_b transitions because we have not, as yet, completed our saturation studies in this transition.[27]

The 1550-cm^{-1} ν_{8a} vibration of tryptophan, which dominates the Raman spectra for excitation throughout the $B_{a,b}$ transition, is also strong with excitation in the L_a and L_b transition. This is the same benzene mode that dominates the spectra of the other substituted benzene derivatives. The assignment of the 1550-cm^{-1} mode to the ν_{8a} benzene mode is consistent with our observed preresonance intensity increases for excitation wavelengths less than 220 nm. This assignment agrees with Hirakawa[39,a] but disagrees with Rava and Spiro[21] and Lautie et al.[59]

The 1614-cm^{-1} band was previously assigned to a vibration with atomic displacements similar to that of the ca. 1636-cm^{-1} b_{3g} naphthalene vibration.[39] We, instead, assign this vibration to the ν_{8b} mode of an ortho-substituted benzene ring. Indeed, the ν_{8b} vibrations of ortho-substituted derivatives occur higher in frequency than the ν_{8a} vibrations.[36c] Furthermore, the enhancement of this vibration by the $B_{a,b}$ transition of tryptophan is similar to the preresonance $B_{a,b}$ enhancement extrapolated for the (1556-cm^{-1}) ν_{8b} vibration of tyrosinate (Figure 7). We do not see evidence for enhancement of the 1614-cm^{-1} mode by the ca. 280-nm transition, in contrast to the results of Hirakawa et al.[39a]

The 1578-cm^{-1} mode appears to be enhanced by the 280-nm transition and by transitions further in the UV above 217 nm.[21] The enhancement by the $B_{a,b}$ state is small for the 1578-cm^{-1} peak. Although not obvious from the Figure 8 excitation profiles because of the ordinate scaling, the intensities of the 1350- and 1578-cm^{-1} modes increase as excitation approaches the 280-nm L_a, L_b absorption bands (see Table IV). These are the only bands to show significant enhancement in the ca. 280-nm absorption band.

Three distinct enhancement patterns are evident from our excitation profile data and the 200-nm tryptophan Raman spectrum of Rava and Spiro.[21]

Pattern 1. The 757-, 1006-, and 1550-cm^{-1} bands show strong enhancement by the 220-nm absorption band and also show preresonance enhancement from transitions located further in the UV. No enhancement by the L_a, L_b transition is observed.

Pattern 2. The 1350- and 1578-cm^{-1} bands show strong enhancement in the far-UV and in the L_a, L_b bands but small enhancement in the $B_{a,b}$ state at 220 nm.

Pattern 3. The intensities of the 877-, 1232-, and 1460-cm^{-1} bands smoothly increase as the excitation wavelength decreases further into the UV.

The 1350-cm^{-1} mode is unique because it appears to directly derive from a pyrrole vibration. It shows frequency shifts upon ^{15}N substitution and NH deuterium substitution.[39a] We suggest that the 1578-cm^{-1} mode also mainly involves pyrrole atomic displacements because it shows an excitation profile similar to that of the 1350-cm^{-1} mode. Those vibrational modes which increase their intensity smoothly (pattern 3) presumably involve both the phenyl and pyrrole groups, while those enhanced mainly in the 220-nm absorption band and further in the UV at 200 nm are predominantly phenyl group based. The *relatively* weak enhancement shown by the ν_{8b} band of tyrosinate with 200-nm excitation in the $B_{a,b}$ absorption band[21] is consistent with our assignment of the 1614-cm^{-1} band of tryptophan to the ν_{8b} vibration.

A selective enhancement of pyrrole based vibrations by the L_a, L_b band is not surprising. The addition of the pyrrole substituent to benzene severely perturbs this absorption band whereas simple *o*-alkyl substitution on benzene perturbs the lowest energy

(59) Yeargers, E. *Biophys. J.* **1968**, *8*, 1505.
(60) Lautie, A.; Lautie, M. F.; Gruger, A.; Fakhri, T. *Spectrochim. Acta, Part A* **1980**, *36A*, 85.

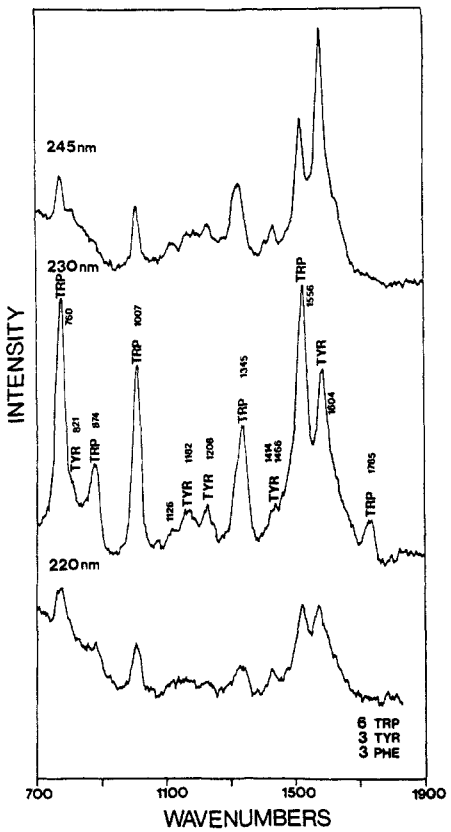

Figure 10. Resonance Raman spectra of chicken egg white lysozyme (M_w = 13 900 g/M) which contains 129 amino acid residues including six tryptophans, three tyrosines, and three phenylalanines. All solutions at pH 6.86. (A) Excitation wavelength = 245 nm. Average power = 2 mW. Lysozyme = 5.0 mg/mL. Spectral resolution = 11 cm^{-1}. (B) Excitation wavelength = 230 nm. Average power = 4 mW. Lysozyme = 5.0 mg/mL. Spectral resolution = 12 cm^{-1}. (C) Excitation wavelength = 220 nm. Average power = 12.5 mW. Lysozyme = 2.5 mg/mL. Spectral resolution = 13 cm^{-1}.

absorption band much less. The oscillator strength of the transition(s) in tryptophan approaches that of an allowed transition. This indicates that much of the oscillator strength derives from the pyrrole group. A less dramatic oscillator strength increase occurs for the $B_{a,b}$ states between 190 and 220 nm. Thus, it is expected that symmetric pyrrole vibrations will be selectively enhanced by the L_a, L_b tryptophan transitions. This argument depends upon the assumption that the magnitude of resonance enhancement scales both with the degree of involvement of a functional group in the transition moment and the relative contribution of the atomic displacements of the functional group to the vibration.

Aromatic Amino Acids in Proteins. The excitation profile data reported here detail the selectivity available for aromatic amino acid protein studies. For example, the 245-nm excited Raman spectrum of lysozyme, a protein with six tryptophans, three tyrosines, and three phenylalanines, shows strong enhancement of tyrosine and tryptophan vibrations (Figure 10). An excitation wavelength shift to 230 nm results in an increase in the relative intensities of the tryptophan peaks because the tryptophan Raman cross sections increase. The tryptophan 1350-cm^{-1} peak intensity increases less than that of the 1006- and 1550-cm^{-1} peaks because the 1350-cm^{-1} excitation profile is less sharply peaked. Although we have not reported tyrosine cross sections in this report, we can estimate them from Figure 10. At 245-nm excitation the lysozyme tryptophan 1006-cm^{-1} peak will have a cross section of ca. 2×10^{-26} cm^2/(molecule sr). Thus, for 245-nm excitation the average tyrosine 1604-cm^{-1} cross section is ca. 1×10^{-25} cm^2/(molecule sr). This compares with a cross section of 3×10^{-25} cm^2/(molecule sr) for tyrosinate. The 1604-cm^{-1} tyrosine cross sections can be similarly estimated to be 7×10^{-25} cm^2/(molecule sr) at 230 nm and 3×10^{-24} cm^2/(molecule sr) at 220 nm.

The ratios between aromatic amino acid excitation profiles can be used to construct selectivity curves for choosing particular aromatic amino acids for study. The 217–300-nm spectral region is especially selective for aromatic amino acids; the peptide backbone vibrations[4] have cross sections of less than 3×10^{-27} cm^2/(molecule sr), while C–C stretching vibrations in saturated aromatic amino acids have cross sections of less than 10^{-27} cm^2/(molecule sr) in this spectral region.[3,4] Selective enhancement of phenylalanine in proteins requires excitation further into the UV.

Raman protein structural studies utilize both frequencies and intensities to monitor environment and interresidue interactions. Photochemistry and saturation phenomena must be avoided because they will cause changes in aromatic amino acid relative intensities and create new spectral features.

Conclusions

Total differential UV resonance Raman excitation profile cross sections have been measured in the 217–600-nm spectral region for the aromatic amino acids. The dominant mechanism for resonance enhancement for aromatic amino acids is via the Franck–Condon Albrecht *A* term. The excitation profiles indicate charge-transfer character in the L_b and $B_{a,b}$ excited states of tyrosinate and detect underlying vibronic structure in the L_a absorption band.

The excitation profile data were used to assign the enhanced tyrosinate and tryptophan vibrations. These aromatic amino acid excitation profiles can be used to predict the selectivity available for aromatic amino acid enhancement in proteins. Photochemical transients and optical saturation phenomena can give rise to artifacts in the Raman spectra of proteins.

Acknowledgment. We gratefully acknowledge partial support of this work from NIH Grant 1R01GM30741-04. Sanford A. Asher is an Established Investigator of the American Heart Association; this work was done during the tenure of an Established Investigatorship of the American Heart Association and with funds contributed in part by the American Heart Association, Pennsylvania affiliate.

Registry No. Phenylalanine, 63-91-2; tyrosine, 60-18-4; tryptophan, 73-22-3; lysozyme, 9001-63-2.